Pathogens and Disease, 74, 2016, ftw008

doi: 10.1093/femspd/ftw008
Advance Access Publication Date: 21 January 2016
Research Article

RESEARCH ARTICLE

Transmembrane segments of complement receptor 3 do not participate in cytotoxic activities but determine receptor structure required for action of *Bordetella* adenylate cyclase toxin

Tomas Wald[1], Adriana Osickova[1,2], Jiri Masin[1], Petra M. Liskova[1,3], Inga Petry-Podgorska[4], Tomas Matousek[4], Peter Sebo[1] and Radim Osicka[1,*]

[1]Institute of Microbiology of the CAS, v. v. i., Videnska 1083, 142 20, Prague 4, Czech Republic, [2]Department of Biochemistry, Faculty of Science, Charles University in Prague, Hlavova 8, 128 43, Prague 2, Czech Republic, [3]Department of Genetics and Microbiology, Faculty of Science, Charles University in Prague, Vinicna 5, 128 44 Prague 2, Czech Republic and [4]Institute of Analytical Chemistry of the CAS, v. v. i., Veveri 97, 602 00 Brno, Czech Republic

*Corresponding author: Institute of Microbiology of the CAS, v.v.i., Videnska 1083, 142 20 Prague, Czech Republic. Tel: +420-241-062-770; Fax: +420-241-062-152; E-mail: osicka@biomed.cas.cz

One sentence summary: Transmembrane segments of the integrin complement receptor 3 are not directly involved in cytotoxic activities of *Bordetella* adenylate cyclase toxin but determine receptor structure required for toxin action.

Editor: Teresa Frisan

ABSTRACT

Adenylate cyclase toxin-hemolysin (CyaA, ACT or AC-Hly) of the whooping cough agent *Bordetella pertussis* penetrates phagocytes expressing the integrin complement receptor 3 (CR3, CD11b/CD18, $\alpha_M\beta_2$ or Mac-1). CyaA translocates its adenylate cyclase (AC) enzyme domain into cell cytosol and catalyzes unregulated conversion of ATP to cAMP, thereby subverting cellular signaling. In parallel, CyaA forms small cation-selective membrane pores that permeabilize cells for potassium efflux, contributing to cytotoxicity of CyaA and eventually provoking colloid-osmotic cell lysis. To investigate whether the single-pass α-helical transmembrane segments of CR3 subunits CD11b and CD18 do directly participate in AC domain translocation and/or pore formation by the toxin, we expressed in CHO cells variants of CR3 that contained artificial transmembrane segments, or lacked the transmembrane segment(s) at all. The results demonstrate that the transmembrane segments of CR3 are not directly involved in the cytotoxic activities of CyaA but serve for maintaining CR3 in a conformation that is required for efficient toxin binding and action.

Keywords: adenylate cyclase toxin; ICP-MS; CD11b/CD18; complement receptor 3; CyaA; transmembrane segment

INTRODUCTION

Bacterial toxins use specific cellular receptors for binding and direct penetration of target cell membranes, or for toxin internalization by receptor-mediated endocytosis. The multifunctional adenylate cyclase toxin-hemolysin (CyaA, ACT or AC-Hly) is a key virulence factor of the whooping cough agent

Received: 30 July 2015; **Accepted:** 17 January 2016

Bordetella pertussis (Weiss *et al.* 1984; Goodwin and Weiss 1990; Khelef, Sakamoto and Guiso 1992). The toxin targets myeloid phagocytes expressing on their surface the integrin complement receptor type 3 (CR3, CD11b/CD18, $\alpha_M\beta_2$ or Mac-1) (Guermonprez *et al.* 2001). CyaA consists of a highly active and cell-invasive N-terminal adenylate cyclase (AC) enzyme domain of ~400 residues that is fused to a covalently palmitoylated pore-forming RTX cytolysin moiety (Hly) of ~1300 residues (Glaser *et al.* 1988a, 1988b; Benz *et al.* 1994; Hackett *et al.* 1994). The latter is composed of a hydrophobic domain (residues 500–700) that participates in membrane translocation of the AC domain and penetrates cellular membrane to form cation-selective membrane pores (Benz *et al.* 1994; Osickova *et al.* 1999; Basler *et al.* 2007). The hallmark feature of the Hly domain is the calcium-binding RTX nonapeptide repeat domain (last 700 residues) that is important for binding of the toxin to CR3 (Glaser *et al.* 1988a, 1988b; El-Azami-El-Idrissi *et al.* 2003). The interaction of CyaA with CR3 is initiated by a low affinity interaction of the toxin with N-linked glycan chains of the CD11b subunit of CR3 (Morova *et al.* 2008; Hasan *et al.* 2015), which is followed by tight binding of the toxin to a segment located at the interface of the β-propeller and thigh domains of CD11b (Osicka *et al.* 2015). Upon binding of CyaA to CR3, the toxin inserts into the cytoplasmic membrane of phagocytes and permeabilizes them for influx of calcium ions. This triggers calpain-mediated cleavage of the actin-anchoring talin tether of CR3, and the integrin-CyaA complex is next recruited into the cholesterol-rich membrane microdomains, from where the AC domain translocation across the plasma membrane is completed (Bumba *et al.* 2010). Once in cell cytosol, the AC domain is activated by binding of the cytosolic calcium-binding protein calmodulin and catalyzes massive and unregulated conversion of the cellular ATP into the key second messenger molecule cAMP (Wolff *et al.* 1980; Confer and Eaton 1982; Greenlee, Andreasen and Storm 1982). In parallel, CyaA permeabilizes the cell membrane by forming small cation-selective pores that enable efflux of intracellular potassium ions (Benz *et al.* 1994; Hewlett, Donato and Gray 2006).

Complement receptor 3 (CR3 or CD11b/CD18) belongs to the single-pass type I transmembrane subfamily of β_2 integrins that are expressed on the surface of polymorphonuclear leukocytes and mononuclear phagocytes (Arnaout 1990). The β_2 integrin family consists of four members sharing a common β subunit (CD18) that associates into heterodimers with four different but structurally homologous α subunits (Tan *et al.* 2000; Campbell and Humphries 2011). Both the α and β subunits consist of long N-terminal extracellular domains that are linked by single-pass transmembrane segments to short C-terminal cytoplasmic tails (Kishimoto *et al.* 1987; Arnaout *et al.* 1988; Corbi *et al.* 1988). The CR3 recognizes molecules found on the surface of invading bacteria and it also binds the iC3b opsonin attached to the surface of foreign cells (Takizawa, Tsuji and Nagasawa 1996; Agramonte-Hevia *et al.* 2002). The activity of CR3 on the cell surface is tightly regulated via bidirectional signaling, so that the integrin ectodomain is kept in a low affinity (bent) state in non-activated cells (Kim, Carman and Springer 2003). Activation of CR3 induces separation of the cytoplasmic tails and the single-pass α-helical transmembrane segments (Kim, Carman and Springer 2003). This is thought to destabilize the headpiece–leg interface on the extracellular side of the heterodimer complex and provokes integrin extension, whereby the I-domain becomes accessible for endogenous ligands (Lu *et al.* 2001; Shimaoka *et al.* 2001). Extension of the integrin receptors can also be induced artificially by introducing specific mutations in the transmembrane segments, causing separation of transmembrane α-helices, or by activation of the extracellular domains (Hughes *et al.* 1996; Luo *et al.* 2005; Vararattanavech *et al.* 2010; Ye, Kim and Ginsberg 2011).

CyaA is a prototypic example of an enzymatically active toxin that can directly translocate across the cytoplasmic membrane of a variety of cells without the need for receptor-mediated endocytosis (Gordon *et al.* 1989; Iwaki, Ullmann and Sebo 1995; Guermonprez *et al.* 1999). The presence of CR3 on cell surface then increases by about two orders of magnitude the cell binding and penetration efficacy of CyaA when compared to cells devoid of CR3. This raises the question whether CR3 only acts as a molecular antenna that increases the local concentration of CyaA on the cellular surface, or whether the single-pass α-helical transmembrane segments of CR3 are directly participating in the translocation of the AC domain and/or toxin pore formation by CyaA. Using CR3 variants fused to artificial transmembrane segments, or lacking the transmembrane segment(s) completely, we show that the transmembrane α-helices of CR3 do not participate in cytotoxic activities of CyaA and that these segments serve for maintaining of a proper conformation of the CR3 complex that is required for toxin binding and action.

MATERIALS AND METHODS

Antibodies

Monoclonal antibody (mAb) OKM1 (mouse IgG2b) specific for human CD11b was purified from the OKM1 hybridoma obtained from the European Collection of Cell Cultures, Porton Down, UK. OKM1 was conjugated with Dyomics 495-NHS ester (Dy-495) (Dyomics GmbH, Jena, Germany) according to the manufacturer's protocol. Anti-human CD11b mAb MEM-174 (mouse IgG2a), anti-human CD18 mAb MEM-48 (mouse IgG1) and allophycocyanin (APC) conjugated mAb MEM-48 were purchased from Exbio, Vestec, Czech Republic. Fluorescein isothiocyanate (FITC) labeled mAb CBRM1/5 (mouse IgG1) specific for human CD11b was obtained from eBioscience, San Diego, CA.

Plasmid constructs

pT7CACT1 was used for coexpression of *cyaC* and *cyaA* genes allowing production of recombinant CyaC-activated CyaA in *Escherichia coli* under control of the isopropyl-β-D-thiogalactopyranoside-inducible *lacZ* promoter (Osicka *et al.* 2000).

Human cDNAs encoding CD11b and CD18 were a kind gift of D. Golenbock, Boston University School of Medcine, Boston, MA (Ingalls *et al.* 1998). The cDNA for CD11b was cloned into the pcDNA3 expression vector (Invitrogen, Carlsbad, CA) and the cDNA for CD18 into the pcDNA3.1/Zeo (+) expression vector (Invitrogen, Carlsbad, CA).

For production of CD11b variants with the replaced transmembrane segments, a nucleotide substitution C2691T was introduced by oligonucleotide-directed PCR mutagenesis into the cDNA for CD11b to generate a new AflII restriction site without altering the coding sequence. Similarly, a new BsiWI restriction site was introduced after the stop codon of the cDNA for CD11b. These restriction sites were then used to construct cDNAs encoding the CD11b variants with the transmembrane segment replaced with artificial sequences (CD11b-$L_{23\text{-}7}$ or CD11b-$V_{6/13E}$), or with a sequence of the decay accelerating factor (DAF; CD11b-GPI). For production of CD18 variants, the naturally occurring

BlpI and EcoRV restriction sites in the cDNA for CD18 were used to construct cDNAs encoding the CD18 variants with the transmembrane segment replaced with artificial sequences (CD18-$L_{23\text{-}7}$ and CD18-$V_{6/13E}$), or with a sequence of the DAF (CD18-GPI), or completely lacking the transmembrane and cytosolic segments (CD18ΔTMC).

Production, purification and labeling of CyaA

CyaA was produced in the *E. coli* strain XL1-Blue (Stratagene, La Jolla, CA) and purified by a combination of ion exchange chromatography on DEAE-Sepharose and hydrophobic chromatography on Phenyl-Sepharose as previously described (Osicka *et al.* 2000).

Oncolumn labeling of CyaA was performed after the DEAE-Sepharose purification step. Protein samples were diluted four times in ice–cold 50 mM Tris-HCl, pH 8.0 containing 1 M NaCl and loaded on Phenyl-Sepharose beads. To label CyaA with Dyomics 647 (Dy-647), the Phenyl-Sepharose column was washed with 50 mM sodium bicarbonate (pH 8.3), and the beads were subsequently resuspended in the same buffer containing Dy647-NHS ester (Dyomics, Jena, Germany) in a concentration to reach a Dy647:protein molar ratio of ∼6:1. Labeling was performed at 25°C for 2 h; the column was washed with 50 mM Tris-HCl (pH 8.0), and labeled proteins were eluted in a buffer containing 50 mM Tris-HCl (pH 8.0) and 8 M urea. The binding, cell-invasive and hemolytic activities of the labeled CyaA protein were determined as described elsewhere (Osicka *et al.* 2000) and were found to be similar (>90%) to those of unlabeled CyaA.

Cells and growth conditions

CHO-K1 Chinese hamster ovary (CHO) cells (ATCC CCL 61) stably transfected with cDNAs encoding the human CD11b/CD18, CD11b-$L_{23\text{-}7}$/CD18-$L_{23\text{-}7}$, CD11b-$V_{6/13E}$/CD18-$V_{6/13E}$, CD11b/CD18ΔTMC or CD11b-GPI/CD18-GPI variants were used in the experiments. The cells were grown in F12K medium (GIBCO Invitrogen, Grand Island, NY) supplemented with 10% fetal calf serum (FCS; GIBCO Invitrogen, Grand Island, NY) and antibiotic antimycotic solution (ATB, 0.1 mg/ml streptomycin, 1000 U/ml penicillin and 0.25 μg/ml amphotericin) (Sigma-Aldrich, St. Louis, MO). The human monocytic cell line, THP-1, was cultured in RPMI 1640 (Sigma-Aldrich, St. Louis, MO) supplemented with 10% FCS and antibiotic antimycotic solution.

Human primary monocytes were isolated from commercial anonymous leukopacks of healthy human blood donors, which were purchased from the Blood Bank of Thomayer Hospital, Prague, Czech Republic, and informed consent was therefore not applicable. Handling of cells of human origin was performed in compliance with the quality and safety requirements of the Act no. 296/2008 Coll. and the decree no. 422/2008 Coll., and the used protocols were in accordance with internal guidelines of the Institute of Microbiology of the CAS, v.v.i. Briefly, content of leukopack was layered over a Ficoll-Paque Plus (GE Healthcare, Uppsala, Sweden) and centrifuged for 30 min at 400 × *g*. Peripheral blood mononuclear cells were removed from the Ficoll–plasma interface, washed three times with a phosphate buffered saline solution and plated in RPMI 1640 medium supplemented with 10% FCS. After 12 h at 37°C, non-adherent cells were washed out from the plate and adherent monocytes were suspended in complete RPMI 1640 medium supplemented with 10% FCS.

Establishment and selection of stably transfected cell lines

Lipofectamine 2000 (Invitrogen, Grand Island, NY) was used for plasmid DNA transfection of CHO cells according to the manufacturer's protocol. Briefly, 0.8 μg of a highly purified plasmid DNA containing a cDNA insert encoding an appropriate CD18 variant (CD18, CD18-$L_{23\text{-}7}$, CD18-$V_{6/13E}$ or CD18-GPI) was mixed with 2 μl of Lipofectamine 2000, both diluted in 50 μl of Opti-MEM I medium (Invitrogen, Grand Island, NY), and the mixture was incubated at 25°C for 20 min. The plasmid DNA: lipofectamine mix was added to CHO cells (> 90% confluency) seeded in 24-well tissue culture plate in F12K medium with 10% FCS and incubated for 6 h at 37°C. The medium was replaced for fresh medium, and the transfected cells were cultured for 24 h and then transferred to F12K medium supplemented with 10% FCS, ATB and 300 μg/ml of zeocin to select for stable transfectants for 10 days. A total of 1×10^6 stably transfected CHO cells were then stained for 30 min at 4°C in 500 μl of cHBSS buffer (HEPES buffered salt solution (HBSS buffer; 10 mM HEPES, pH 7.4, 140 mM NaCl, 5 mM KCl) complemented with 2 mM $CaCl_2$, 2 mM $MgCl_2$, 1% (w/v) glucose and 1% (v/v) FCS) containing the anti-CD18 MEM-48 mAb (at an 1:50 dilution). MEM-48 positive CHO cells expressing high levels of the CD18 variants were isolated from the pool of transfected cells using a FACS Vantage cell sorter (Becton Dickinson, Franklin Lakes, NJ) into individual wells of 6-well plate containing F12K medium supplemented with 10% FCS and ATB.

CHO cells expressing the CD18 variants were further transfected with highly purified plasmid DNA containing a cDNA insert encoding an appropriate CD11b variant (CD11b, CD11b-$L_{23\text{-}7}$, CD11b-$V_{6/13E}$, or CD11b-GPI). The cells were grown in F12K medium supplemented with 10% FCS, ATB, 600 μg/ml of G418 and 300 μg/ml of zeocin to select for stable double-transfected cells for 10 days. A total of 1×10^6 cells were then stained for 30 min at 4°C in 500 μl of cHBSS buffer containing the OKM1 (at an 1:200 dilution from a stock solution of a concentration 5.2 mg/ml) and MEM-48 (1:50) mAbs. Individual cells expressing high levels of the CD11b and CD18 variants were isolated from cell population using a FACS Vantage cell sorter into individual wells of 96-well plates. After 3 weeks, the cells from positive wells were expanded, and 1×10^5 cells were then stained for 30 min at 4°C in 50 μl of cHBSS buffer containing the OKM1 (1:200) and MEM-48 (1:50) mAbs. CHO clones expressing on the cell surface, the same amounts of the integrin variants, were selected by FACS analysis and used for further experiments. To monitor that the expression of the integrin variants on the cell surface of CHO clones remained unchanged, the amounts of integrin molecules were systematically quantified in each experiment by staining with the OKM1 and MEM-48 mAbs.

For establishment of CHO cells expressing the CD11b/CD18ΔTMC variant, CHO cells stably expressing intact CD11b (Morova *et al.* 2008; Hasan *et al.* 2015) were transfected with a plasmid DNA containing a cDNA insert encoding the CD18ΔTMC integrin variant, and the double-transfected cells were further established as described above.

Analysis of mAb, fibrinogen and CyaA binding to transfected cells by flow cytometry

For staining of integrin molecules with mAbs, 1×10^5 stably transfected CHO cells were incubated for 30 min at 4°C in 50 μl of cHBSS buffer containing the fluorescently labeled OKM1 (1:200), MEM-48 (1:50) or CBRM1/5 (1:50) mAbs.

For fibrinogen-binding assay, 1×10^5 CHO cells expressing integrin molecules were incubated for 30 min at 4°C in 100 μl of cHBSS buffer containing 10 μg/ml of fibrinogen (Sigma-Aldrich, St. Louis, MO) conjugated with Dy495 according to the manufacturer's protocol.

For CyaA-binding assay, 1×10^5 CHO cells expressing integrin molecules were incubated for 30 min at 4°C in 50 μl of cHBSS buffer containing different concentrations of CyaA conjugated with Dy647.

To analyze mAb, fibrinogen and CyaA binding, the cells were washed, resuspended in HBSS and analyzed by flow cytometry on a FACS LSR II instrument (BD Biosciences, San Jose, CA) in the presence of 1 μg/ml of Hoechst 33258. Data were analyzed by FlowJo software (Tree Star, Ashland, OR), and appropriate gatings were used to exclude cell aggregates and dead cells.

To block CyaA binding to intact CR3 and its mutant variants, 1×10^5 integrin-transfected CHO cells were pre-incubated without or with CyaA-blocking anti-CD11b OKM1 mAb (1:200) in 50 μl of cHBSS for 30 min at 4°C. The unbound mAb was removed by three washes with cHBSS, and the cells were subsequently incubated with different concentrations of CyaA in 100 μl of cHBSS for 30 min at 4°C. The unbound toxin was washed out and the cells were analyzed by flow cytometry.

Immunoprecipitation

A total of 4×10^6 CHO cells expressing intact CR3 or its mutant variants were lysed with 1 ml of Triton lysis buffer [50 mM Tris-HCl (pH 7.4), 150 mM NaCl, 1% Triton X-100 and EDTA-free protease inhibitor mixture (Roche Applied Science, Penzberg, Germany)] for 30 min on the roller shaker at 4°C. The lysate was centrifuged for 15 min at 12 000 × g at 4°C and the supernatant was transferred to a fresh tube on ice. The anti-CD11b mAb MEM-174 covalently linked to agarose beads (20 μl) was added to the supernatant and the samples were incubated on a roller shaker for 3 hours at 4°C. The beads were washed five times with 1 ml of lysis buffer, mixed with 60 μl of elution buffer (50 mM Tris-HCl (pH 7.4), 10% SDS) and pelleted for 5 s at 12 000 × g. The immunoprecipitated proteins in supernatants were separated by 7.5% SDS/PAGE, transferred to a nitrocellulose membrane, probed by the anti-CD18 mAb MEM-48 (at a final concentration of 1 μg/ml) and revealed by peroxidase-conjugated secondary antibody (1:2,500) by using the chemiluminescence detection system (ECL; GE Healthcare, Little Chalfont, UK).

Confocal microscopy

A total of 5×10^4 CHO cells expressing intact CR3 or its mutant variants were let to adhere on glass bottom microwell dishes (MatTek, Ashland, OR) for 30 min, washed with HBSS and coincubated with the OKM1 (1:200) and MEM-48 (1:50) mAbs for 10 min at 37°C. Cells were washed with HBSS, and images were captured using an Olympus confocal microscope FV1000 with a UPLSAPO 20x, NA 0.75 objective. Quantification of CD11b and CD18 colocalization on the surface of CHO transfected cell lines was performed using the FV10-ASW 2.0 Viewer software. Individual cells were selected as regions of interest (ROIs), and Pearson's correlation coefficient (Pcc) for each ROI was calculated for the given channels. Average Pcc ± standard deviation (SD) of all analyzed ROIs was calculated. A value of one represents perfect correlation, zero represents random localization.

Determination of intracellular cAMP levels by ELISA

Integrin-transfected CHO cells (5×10^4) were incubated with CyaA at concentrations of 25, 50 and 75 ng/ml for 30 min at 37°C in D-MEM; the reaction was stopped by addition of 0.2% Tween-20 in 100 mM HCl; samples were boiled for 15 min at 100°C, neutralized by addition of 150 mM unbuffered imidazole, and cAMP levels were determined as described previously (Karimova *et al.* 1998).

Analysis of CyaA binding and cell-invasive AC by determination of AC activity

To measure CyaA binding, the integrin-transfected CHO cells (1×10^6) were incubated in DMEM with different concentrations of CyaA for 5 min at 37°C. One-half aliquot was taken, unbound toxin was removed by four washes with DMEM and cell-bound CyaA was quantified by determining AC activity. The other one-half aliquot was treated with trypsin (2 μg/ml) for 10 min at 37°C, followed by the addition of an excess of trypsin inhibitor (4 μg/ml). Cell-invasive AC was measured as the AC protected against externally added trypsin upon internalization into cells by determining AC activity.

AC activity was measured as described previously in the presence of 1 mM calmodulin (Ladant 1988). Cells were lysed with 0.1% Triton X-100 for determination of cell-bound or cell-invasive AC enzyme activity. Cell pellet was incubated at 30°C with 50 μl of a mix containing 60 mM Tris-HCl (pH 8.0), 7 mM $MgCl_2$, 0.1 mM $CaCl_2$, 0.1% (w/w) Triton X-100, 2 mM [α-^{32}P]ATP, 1 mg/ml BSA, 0.1 mM [2,8-^{3}H]cAMP and 1 μM calmodulin. The reaction was stopped by addition 200 μl of 0.5 M HCl, and the samples were heated for 5 min at 100°C. The samples were neutralized by the addition of 1.5 M unbuffered imidazole (200 μl), and the cAMP was separated on aluminium oxide column by elution with 10 mM imidazole (pH 7.6). The radioactivity in the sample was determined by scintillation counting (Wallac 1409 DSA, Perkin Elmer). One unit of AC corresponds to 1 μmol of cAMP formed in 1 min at 30°C and pH 8.0.

Determination of cytosolic potassium levels by ICP–MS

Determination of cytosolic potassium levels was done according to a previously described protocol (Wald *et al.* 2014). Briefly, 5×10^5 cells were washed three times with 10 ml of cold modified HBSS (mHBSS; 10 mM HEPES, pH 7.4, 145 mM NaCl, 2 mM $CaCl_2$, 2 mM $MgCl_2$ and 1% (w/v) glucose). Incubation of cells with the indicated working concentrations of CyaA was carried out for 4 and 8 min at 37°C. The cells were then washed twice with mHBSS and lysed with 500 μl of deionized water. The lysed cells were centrifuged (20 min, 4°C, 40,000 g, F-20/MICRO, Thermo Fischer Scientific, Waltham, MA) to remove the membranes and the soluble fraction was stored at −20°C. Determination of cytosolic potassium levels by inductively coupled plasma mass spectrometry (ICP-MS) was carried out using an Agilent 7700x inductively coupled plasma mass spectrometer with ASX-500 autosampler, equipped with a Micro-Mist concentric nebulizer and high matrix interface. Potassium was detected at m/z 39, in a collision cell mode (He 4.8 ml/min), using 45Sc and 89Y as internal standards to correct sensitivity drifts. A rinse with 2% HNO_3 and deionized water was inserted between samples. Quantification was performed using a five-point external calibration (0.1–2.0 mg/l K^+). Calibration standards were prepared from a 1000 mg/l K^+ stock solution (VWR, Randor, PA) in deionized water for

lysed pellet samples. Results were processed using Agilent Mass Hunter software.

Statistical analysis

Results were expressed as the arithmetic mean ± SD of the mean. Student´s *t*-test was used to calculate statistical significance when two groups were compared. To test more than two groups, statistical analysis was performed by one-way ANOVA followed by Dunnett's post-test, comparing all the samples with the control. GraphPad Prism 6.0 (GraphPad Software) was used to perform statistical analysis. Significant differences are indicated by asterisks (*, $P < 0.05$; **, $P < 0.01$; ***, $P < 0.001$; ****, $P < 0.0001$).

RESULTS

Amino acid composition of the transmembrane segments of CR3 has no impact on biological activities of CyaA

To examine the involvement of the transmembrane segments of CR3 in the cell-invasive and pore-forming activities of CyaA, we constructed CR3 variants containing artificial transmembrane α-helices (Fig. 1a). To ensure the correct anchoring of the CR3 variants in cell membrane and to preserve the dimerization of the CD11b and CD18 subunits of CR3, the transmembrane segments of CD11b and CD18 were replaced with artificial motifs previously shown to form dimers in the hydrophobic environment (Lemmon *et al.* 1994; Dosch and Ballmer-Hofer 2010). In the constructed CD11b-$L_{23\text{-}7}$/CD18-$L_{23\text{-}7}$ variant, each original transmembrane segment was replaced with a polyleucine stretch containing the dimerization sequence motif L-I-x-x-G-V-x-x-G-V-x-x-T (Fig. 1a) (Lemmon *et al.* 1994). In the second CR3 variant, CD11b-$V_{6/13E}$/CD18-$V_{6/13E}$, the original transmembrane segments were replaced with a polyvaline motif containing two negatively charged glutamate residues (Fig. 1a) (Dosch and Ballmer-Hofer 2010). As documented by flow cytometry analysis (Figs 1b and c), the generated transfected CHO cells stably expressed highly comparable amounts of the CD11b and CD18 subunits of the CD11b-$L_{23\text{-}7}$/CD18-$L_{23\text{-}7}$, CD11b-$V_{6/13E}$/CD18-$V_{6/13E}$ or intact CD11b/CD18 molecules on the surface of transfected cells, respectively. As further documented by confocal microscopy in Fig. S1 (Supporting Information), the mutant CD11b and CD18 subunits colocalized on the surface of cells to the same extent as the intact CR3 subunits, indicating that the mutant subunits still formed heterodimers, like the intact integrin subunits. Indeed, intact as well as mutant CD18 subunits could be immunoprecipitated with the anti-CD11b mAb (MEM-174) from lysates of cells expressing intact or mutant CR3 integrin variants (Fig. 1d). Moreover, the amounts of CR3 expressed on the surface of transfected CHO cells were comparable to the levels of surface-expressed CR3 on the cultured human monocytic THP-1 cells or primary human monocytes that naturally express the CR3 integrin (Fig. S2, Supporting Information). All these results, hence, confirmed that the CHO-expressed CR3 variants were suitable for analysis of the role of their transmembrane segments in CyaA toxin action, as outlined below.

The capacity of cells expressing the CR3 variants to bind CyaA was measured by flow cytometry. As shown in Figs 2a and b and Fig. S3 (Supporting Information), both CHO cell lines expressing the mutant integrins bound CyaA with similar efficacy as the cells expressing the intact CR3. Next, the susceptibility of cells to CyaA penetration and enzymatic intoxication by cAMP formed by the delivered AC domain was determined as intracellular accumulation of cAMP using ELISA. As documented in (Fig. 2c), following exposure to CyaA, comparable levels of cAMP accumulated in cells expressing the mutant integrins and the intact CR3.

To assess whether the transmembrane segments of CR3 participate in pore-forming activity of CyaA, cells were incubated with the toxin, and the efflux of intracellular potassium ions was measured by inductively coupled plasma mass spectrometry (Wald *et al.* 2014). As summarized in Fig. 2d, by difference to cells lacking the CR3 integrin, toxin treatment of CHO cells expressing the intact CR3 provoked rapid efflux of cellular potassium ions, causing a drop of intracellular potassium levels over time down to nearly 50% of the initial content. A similar decrease of intracellular potassium level was observed upon toxin treatment of cells expressing the CD11b-$L_{23\text{-}7}$/CD18-$L_{23\text{-}7}$ or CD11b-$V_{6/13E}$/CD18-$V_{6/13E}$ variants, respectively (Fig. 2d).

All these data demonstrate that the swapping of the α-helical transmembrane segments of CR3 for the artificial single-pass and dimer-forming α-helical segments did not affect any of the cytotoxic activities of CyaA. This demonstrates that CyaA upon recognition of the CR3 receptor penetrates the cells, translocates its AC domain across the membrane and forms membrane pores independently of the amino acid composition of the transmembrane segments of CR3.

CR3 variants lacking the transmembrane segment(s) bind CyaA with lower efficacy and are inefficient in supporting toxin activities of CyaA

To corroborate the above-described observations, we constructed CR3 variants lacking either one or both transmembrane segments of the CD11b and CD18 subunits (Fig. 3a). First, we established a CHO-CD11b/CD18ΔTMC cell line stably expressing intact CD11b in a heterodimer with a CD18 subunit that is devoid of the transmembrane and cytosolic segments. We failed, however, to establish a cell line expressing the heterodimer of an intact CD18 subunit with a CD11b subunit lacking the transmembrane and cytosolic segments. Therefore, CHO cells were constructed that expressed a CR3 variant with the transmembrane and cytosolic segments of both CD11b and CD18 replaced with the 37 residue-long sequence of the DAF (Fig. 3a). This was used because the last 28 residues of DAF are replaced during post-translational modification by a glycosyl-phosphatidylinositol (GPI) anchor, which was previously shown to attach the ectodomain of CR3 to the plasma membrane (Moran *et al.* 1991). As shown by flow cytometry analysis (Figs 3b and c) and confocal microscopy (Fig. S1, Supporting Information), the CHO-CD11b/CD18ΔTMC, CHO-CD11b-GPI/CD18-GPI and control CHO-CD11b/CD18 cells expressed highly comparable amounts of both CD11b and CD18 subunits on cell surface. Using the coimmunoprecipitation method described above, we confirmed that the CR3 variants lacking the transmembrane segment(s) still formed stable heterodimers as the intact integrin (Fig. 3d).

It was previously shown that deletion of the transmembrane and cytoplasmic segments of the CD18 subunit of the integrin CD11a/CD18 (Tan *et al.* 2000), or attaching of the CD11a/CD18 ectodomain to the plasma membrane via the GPI anchor, results in exposure of an extended (high-affinity) conformation of the integrin on cell surface (Pyszniak, Carpenito and Takei 1997). To investigate whether also the here-constructed mutant variants of CR3 were in the extended conformation, we

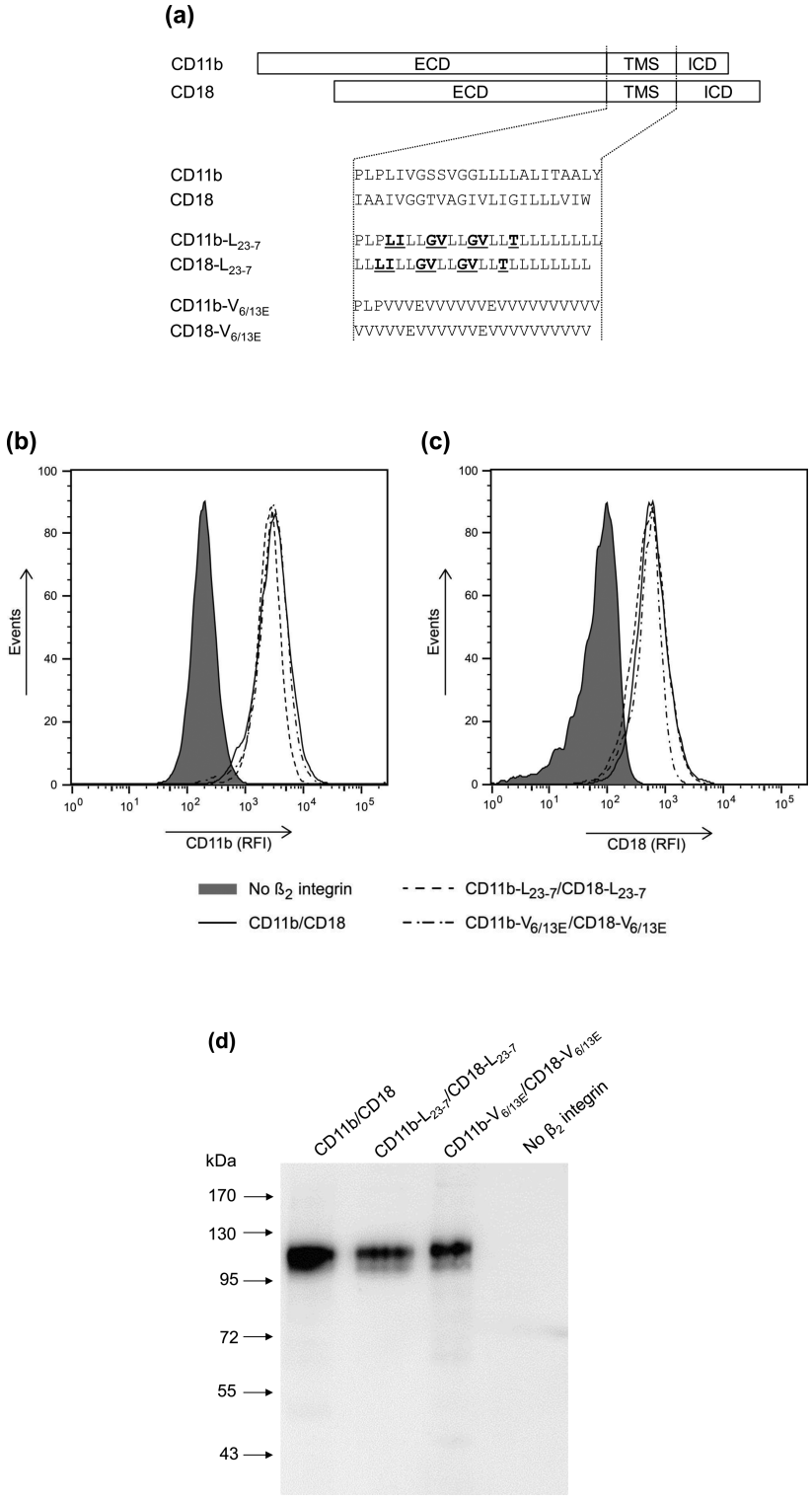

Figure 1. Cell surface expression of CR3 variants with artificial transmembrane segments. (**a**) Schematic map of the CD11b and CD18 subunits of CR3 and the amino acid composition of their native (CD11b/CD18) and artificial (CD11b-$L_{23\text{-}7}$/CD18-$L_{23\text{-}7}$ or CD11b-$V_{6/13E}$/CD18-$V_{6/13E}$) transmembrane segments. ECD, N-terminal extracellular domain; TMS, single-pass transmembrane segment; ICD, C-terminal cytoplasmic tail. Conserved residues of the L-I-x-x-G-V-x-x-G-V-x-x-T motif are underlined and shown in bold. (**b** and **c**) The α-helical transmembrane segments of CR3 were replaced with artificial dimer-forming α-helices, and the mutant integrins were stably expressed on the surface of CHO cells. The expression of the CD11b (b) and CD18 (c) subunit variants on the cell surface was examined by flow cytometry upon staining of 1×10^5 cells with the anti-CD11b mAb OKM1 (b) or the anti-CD18 mAb MEM-48 (c). A typical overlay flow cytometry histogram from one representative binding experiment out of 16 performed is given. RFI, relative fluorescence intensity. (**d**) The intact CD11b/CD18 integrin or its mutant variants were immunoprecipitated from CHO cell lysates by using the CD11b-specific mAb MEM-174 covalently linked to agarose beads. Upon elution, the samples were separated by SDS/PAGE (7.5%), transferred to a nitrocellulose membrane and immunodetected by the MEM-48 mAb selectively recognizing the CD18 subunit. CHO cells transfected with an empty vector and expressing no β_2 integrin were processed in parallel and used as negative control.

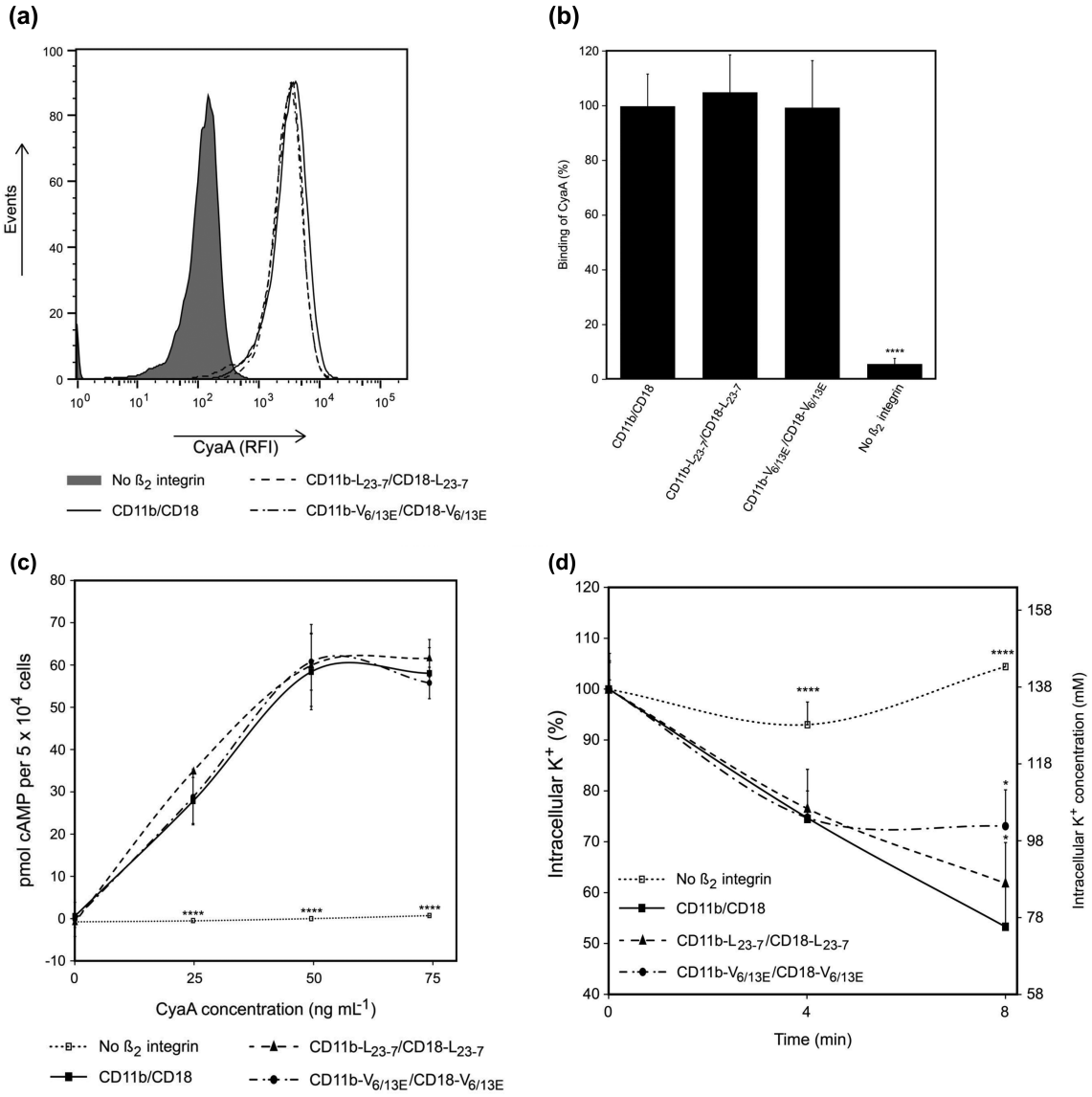

Figure 2. Amino acid composition of the transmembrane segments of CR3 has no impact on biological activities of CyaA. (**a**) 1×10^5 integrin-transfected CHO cells were incubated with 1 μg/ml of CyaA-Dy647, and the cells were analyzed by flow cytometry. A typical overlay histogram from one representative CyaA-binding experiment out of 12 performed is shown. (**b**) CyaA-binding data were deduced from the mean fluorescence intensities of 12 independent flow cytometry experiments and the mean values with SD were expressed as percentage of CyaA binding to CHO-CD11b/CD18 cells. Significantly reduced binding of CyaA to cells expressing no β_2 integrin in comparison with intact CD11b/CD18 is indicated (****, $P < 0.0001$; ANOVA). (**c**) 5×10^4 integrin-transfected CHO cells were incubated with different concentrations of CyaA, and the amounts of accumulated cAMP were determined in cell lysates by ELISA. Each point represents the mean value ± SD of 12 independent experiments. Significant differences between mean values of cAMP intoxication of cells expressing intact CD11b/CD18 and cells expressing no β_2 integrin are shown (****, $P < 0.0001$; ANOVA). (**d**) 5×10^5 transfected CHO cells were incubated with 500 ng/ml of CyaA for 4 and 8 min in HBSS buffer without KCl. The cells were pelleted by centrifugation, washed and lysed by deionized water. Lysates were diluted with deionized water, and the amount of intracellular K^+ was measured by ICP–MS. Each point represents the mean value with SD of at least two independent experiments performed in triplicates. Significant differences between mean values of intracellular potassium ions in cells expressing intact CD11b/CD18 and mutant integrins are shown (****, $P < 0.0001$; *, $P < 0.05$; ANOVA). The level of intracellular potassium ions in cells treated for 8 min without CyaA was taken as 100%. CHO cells expressing no β_2 integrin were processed in parallel and used as negative control (all panels).

used a conformation-dependent mAb, CBRM1/5, which preferentially recognizes the extended conformation of CR3 (Oxvig, Lu and Springer 1999). As shown in Fig. 4a, CHO cells expressing CD11b/CD18ΔTMC or CD11b-GPI/CD18-GPI, respectively, bound the CBRM1/5 mAb ~20- and 30-times more efficiently than cells expressing the intact CR3. To test the functionality of the CR3 mutant variants, cells were treated with fluorescently labeled fibrinogen, a natural ligand of CR3 that is known to bind the extended conformation of CR3 (Diamond and Springer 1993; Diamond *et al.* 1993). As shown by flow cytometry analysis (Fig. 4b), fibrinogen bound both CR3 variants ~3-times more efficiently than the intact integrin. All these data demonstrate that the CD11b/CD18ΔTMC and CD11b-GPI/CD18-GPI variants are exposed on cell surface as heterodimers in the extended conformation and bound fibrinogen, a natural ligand of CR3.

The capacity of cells expressing the CR3 variants to bind CyaA was then assessed by flow cytometry, showing that the mutant variants bound the toxin with a considerably reduced capacity, as compared to cells expressing intact CR3 (Fig. 5a). However, as shown in Fig. 5a, binding of CyaA to the CD18ΔTMC

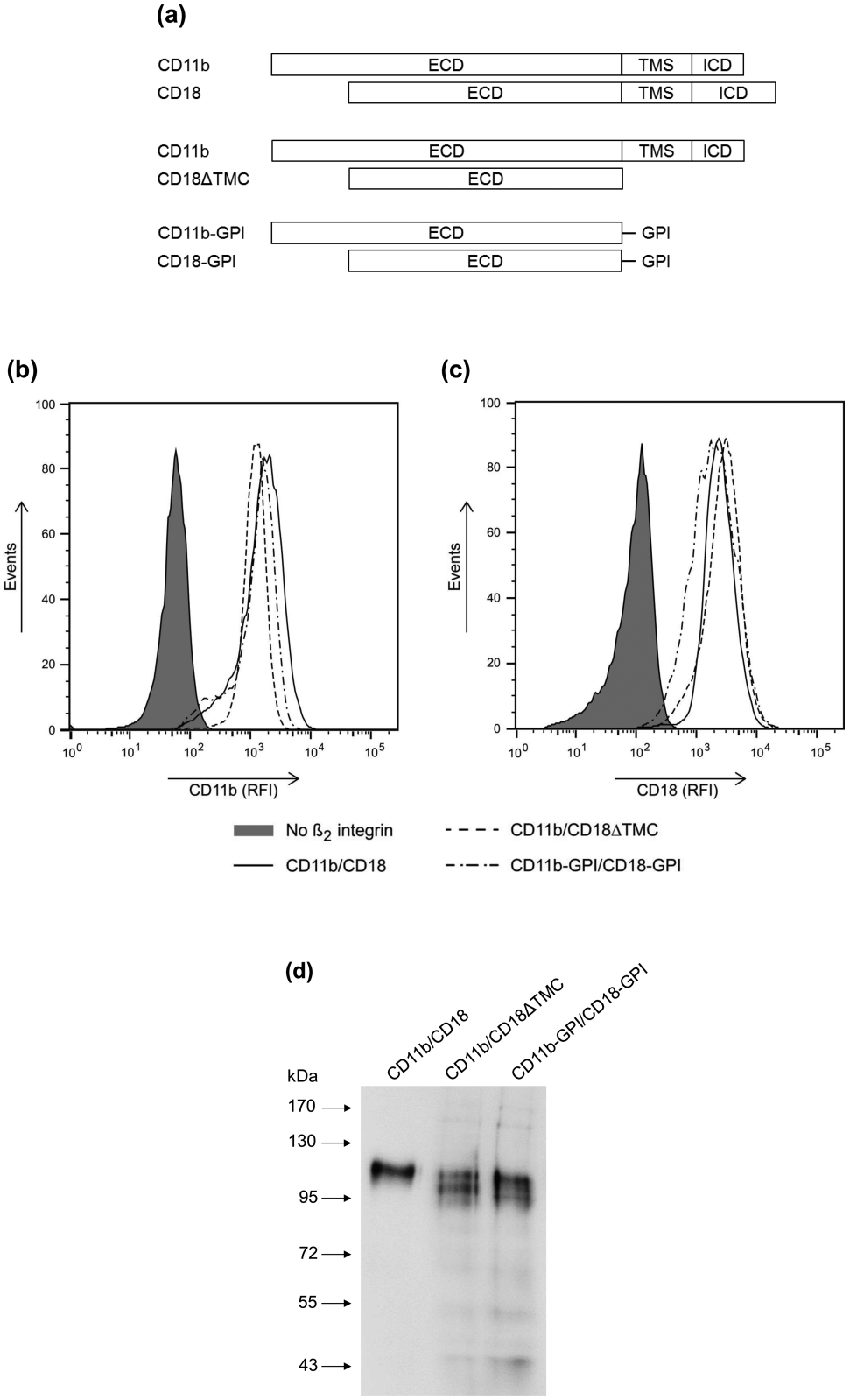

Figure 3. Cell surface expression of CR3 variants lacking one or both transmembrane segments. (**a**) Schematic map of the CD11b and CD18 subunits of intact CR3 and its mutant variants. ECD, TMS and ICD, see the legend to Fig. 1a; GPI, glycosyl-phosphatidyl-inositol anchor. (**b** and **c**) The expression of the CD11b (b) and CD18 (c) subunit variants on the surface of stably transfected CHO cells was examined by flow cytometry upon staining of 1×10^5 cells with the anti-CD11b mAb OKM1 (b) or the anti-CD18 mAb MEM-48 (**c**). CHO cells expressing no β_2 integrin were processed in parallel and used as negative control. A typical overlay flow cytometry histogram from one representative binding experiment out of 12 performed is given. RFI, relative fluorescence intensity. (**d**) The intact CD11b/CD18 integrin and its mutant variants were immunoprecipitated from CHO cell lysates by using the CD11b-specific mAb MEM-174 covalently linked to agarose beads. Upon elution, the samples were separated by SDS/PAGE (7.5%), transferred to a nitrocellulose membrane and immunodetected by the MEM-48 mAb selectively recognizing the CD18 subunit.

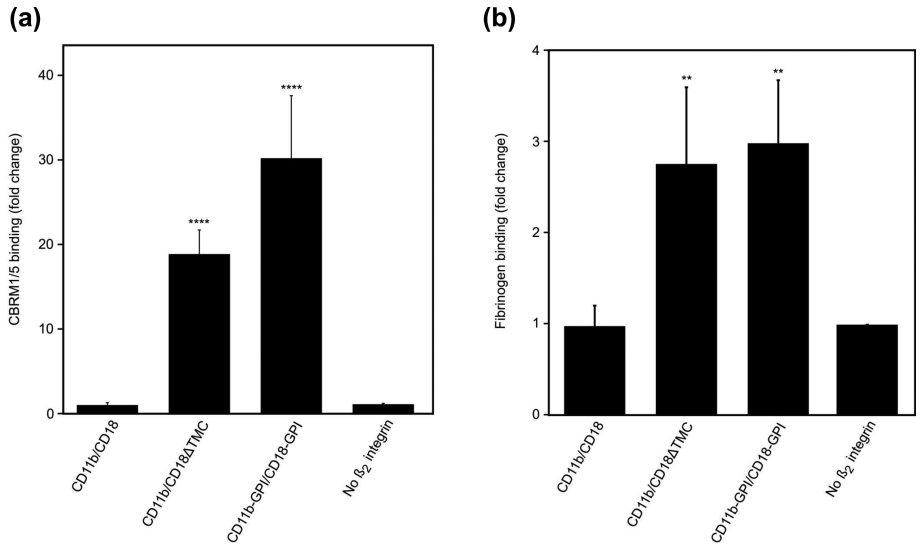

Figure 4. CR3 variants lacking the transmembrane segment(s) bind the conformation-dependent mAb CBRM1/5 and endogenous ligand fibrinogen more efficiently than the intact integrin. (**a** and **b**) 1×10^5 integrin-transfected CHO cells were incubated with the conformation-dependent mAb CBRM1/5 (a) or with fluorescently labeled fibrinogen (b), and the cells were analyzed by flow cytometry. The CBRM1/5 (a) and fibrinogen (b) binding data were deduced from the mean fluorescence intensities of four independent experiments performed in triplicates (CBRM1/5) or three independent experiments (fibrinogen), respectively, and the mean values with SD were expressed as fold change with respect to cells expressing intact CD11b/CD18. Significant differences between mean values of CBRM1/5 or fibrinogen binding to cells expressing intact CD11b/CD18 and mutant integrins are shown (****, $P < 0.0001$; **, $P < 0.01$; ANOVA). CHO cells expressing no β_2 integrin were processed in parallel and used as negative control.

and CD11b-GPI/CD18-GPI variants of CR3 was specific, as it was efficiently blocked by the OKM-1 mAb that recognizes the same segment of CD11b as CyaA (Osicka *et al.* 2015). We next determined whether the CR3 variants with decreased specific toxin-binding capacity would support CyaA action when loaded with the toxin at higher concentrations. As shown in Fig. 5b, to achieve binding of equal amounts of CyaA to cells expressing the intact and the mutant integrins, the toxin concentration used for loading of the mutant integrins had to be increased ~8-times for CHO-CD11b-GPI/CD18-GPI cells or 10-times for CHO-CD11b/CD18ΔTMC cells, respectively.

To determine the amount of CyaA, which would translocate the same amount of AC enzyme when interacting with CD11b-GPI/CD18-GPI or CD11b/CD18ΔTMC, instead of CD11b/CD18, cells expressing the mutant integrins were incubated with a range of concentrations of CyaA. The amount of AC enzyme translocated into the cell cytosol was then determined as the amount of AC that was protected against inactivation by extracellularly added trypsin (Sebo *et al.* 1995; Osickova *et al.* 1999). As shown in Fig. 5c, ~30- and 50-times higher concentrations of CyaA had to be added to cells expressing CD11b-GPI/CD18-GPI or CD11b/CD18ΔTMC, respectively, in order to obtain similar amounts of AC domain translocated as with the cells harboring the intact CR3.

Further, we analyzed the pore-forming capacity of CyaA upon compensating for low efficacy of CyaA binding by an increase of the toxin-loading concentration. As shown in Fig. 5d, CyaA at a concentration of 500 ng/ml did not provoke any potassium efflux from cells expressing the mutant integrins, by difference to toxin action on cells harboring the intact CR3. Nevertheless, as shown in Fig. 5e, incubation with 8000 ng/ml of CyaA provoked a comparable potassium efflux from cells harboring the mutant integrins, as did elicit a toxin concentration of 200 ng/ml on cells expressing the intact integrin.

Taken together, cells expressing the intact CR3 bound CyaA much more efficiently than cells expressing the integrin lacking the CD18 transmembrane segment, or the integrin with both transmembrane segments replaced with the GPI anchor. Nevertheless, when high CyaA amounts were used to compensate for decreased toxin binding efficacy and the toxin amounts bound to cells expressing the mutant integrins reached the amounts bound by cells expressing the intact integrin, the cells expressing the mutant CR3 variants were still susceptible to both cytotoxic activities of CyaA.

DISCUSSION

Binding to cellular receptors allows bacterial toxins to accumulate on cellular surface in the proximity of the plasma membrane, thus facilitating membrane penetration or internalization of the toxin. Through highly specific binding, the receptors ensure concentration of the toxin molecules from the solution into the 2D space of the plasma membrane, increasing the local toxin concentration by at least one order of magnitude. This enables positioning of the toxin molecules in respect to the lipid bilayer of the membrane. These specific and coordinated processes then allow highly effective cytotoxic activities of bound toxins towards target cells. Many bacterial toxins were reported to insert into receptor-free artificial lipid bilayer membranes (Donovan *et al.* 1981; Kagan, Finkelstein and Colombini 1981; Blaustein *et al.* 1989; Schmid *et al.* 1994), or into cells lacking natural proteinaceous receptors. This, however, typically occurs with very low efficacy, as is also the case of CyaA (Gordon *et al.* 1989; Iwaki, Ullmann and Sebo 1995; Guermonprez *et al.* 1999).

It remains poorly defined how the CyaA toxin penetrates the plasma membrane of cells to deliver its enzymatic AC domain into the cytoplasmic space of target cells and how it forms the cation-selective pores. An intriguing question was if CyaA utilizes the transmembrane segments of the CR3 receptor for the induction of the cytotoxic effects. Previously it was shown that diphtheria toxin (DT) of *Corynebacterium diphtheriae* translocates its A fragment across the plasma membrane independently of

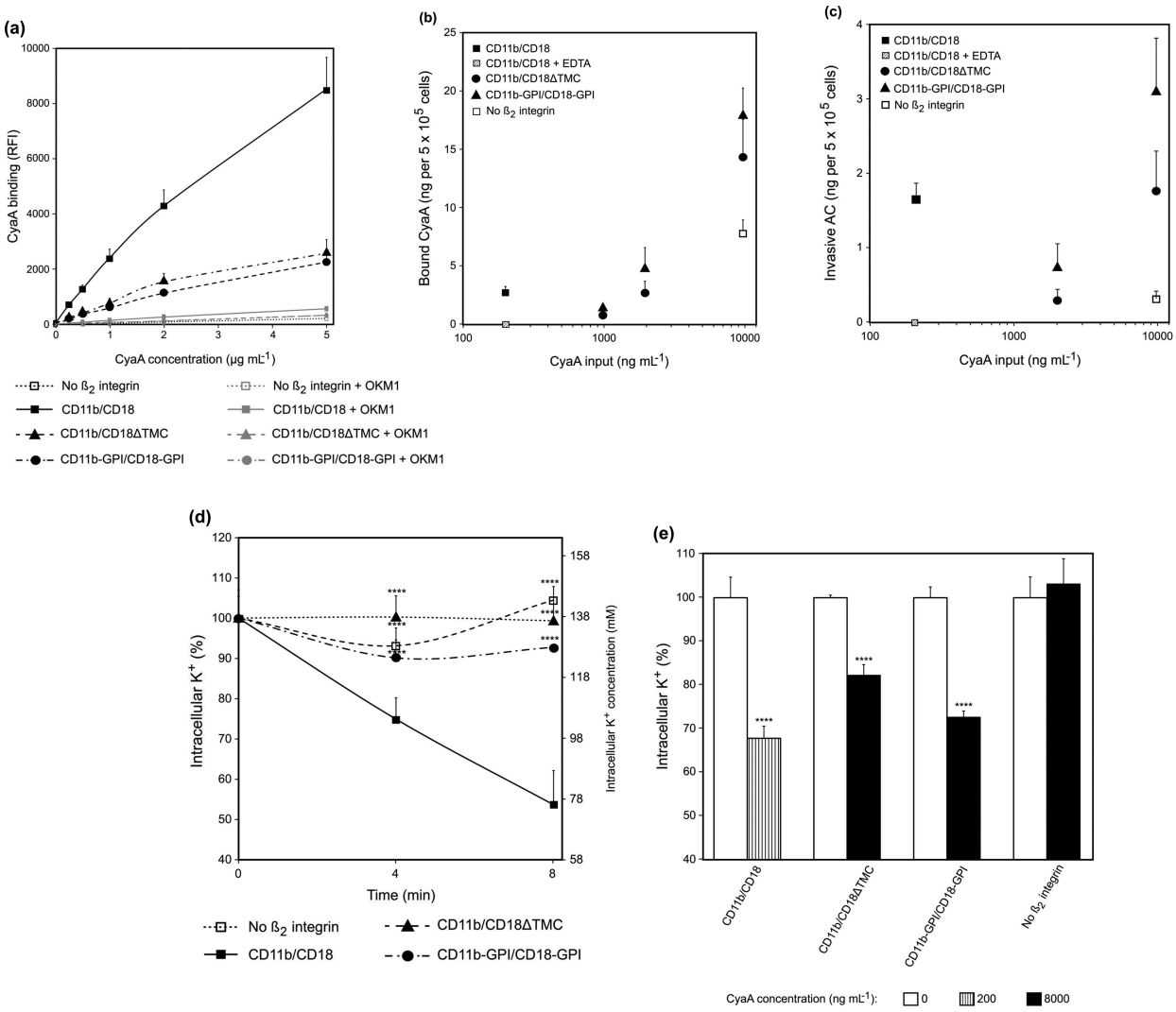

Figure 5. CR3 variants lacking the transmembrane segment(s) bind CyaA with lower efficacy, but still support the biological activities of the toxin. (**a**) 1×10^5 integrin-transfected CHO cells were pre-incubated without or with CyaA-blocking anti-CD11b OKM1 mAb and subsequently treated with different concentrations of CyaA-Dy647. The cells were analyzed by flow cytometry and the mean fluorescence intensities of toxin binding were plotted against the concentrations of CyaA. Each point represents the mean value with SD of three independent experiments. Binding of CyaA to cells expressing CD11b/CD18ΔTMC, CD11b-GPI/CD18-GPI or no β_2 integrin was at all measured toxin concentrations significantly lower than toxin binding to cells expressing intact CD11b/CD18 (****, $P < 0.0001$; ANOVA). Binding of CyaA to cells expressing intact CD11b/CD18 or its mutant variants was in the presence of the OKM1 mAb at all measured toxin concentrations significantly lower than toxin binding to cells expressing intact CD11b/CD18 or its mutant variants in the absence of the OKM1 mAb (at least **, $P < 0.01$; Student´s *t*-test). (**b**) CyaA binding to 5×10^5 integrin-transfected CHO cells was quantified by determination of cell associated AC enzyme activity of the toxin. Since CyaA folding and receptor interaction depends on the presence of calcium ions, CHO cells expressing intact CD11b/CD18 were incubated with CyaA in the presence of EDTA and used as negative control. Each point represents the mean value with SD of two independent experiments performed in duplicates. (**c**) 5×10^5 integrin-transfected CHO cells were incubated with different concentrations of CyaA. The amount of AC enzyme translocated across the cytoplasmic membrane into the cell cytosol was determined as the amount of AC that was protected against inactivation by extracellularly added trypsin. Each point represents the mean value with SD of two independent experiments performed in duplicates. (**d**) 5×10^5 transfected CHO cells were incubated with 500 ng/ml of CyaA for 4 and 8 min, and the levels of intracellular potassium ions were measured as described in the legend to Fig. 2d. Each point represents the mean value with SD of at least two independent experiments performed in triplicates. Significant differences between mean values of intracellular potassium ions in cells expressing intact CD11b/CD18 and mutant integrins are shown (****, $P < 0.0001$; ANOVA). (**e**) 5×10^5 transfected CHO cells were incubated with 0, 200 or 8000 ng/ml of CyaA for 8 min, and the levels of intracellular potassium ions were measured as described in the legend to Fig. 2d. Each bar represents the mean value with SD of at least two independent experiments performed in triplicates. Significant differences between mean values of intracellular potassium ions in cells incubated in the absence or in the presence of CyaA are shown (****, $P < 0.0001$; Student´s *t*-test). The level of intracellular potassium ions in cells treated for 8 min without CyaA was taken as 100%. CHO cells expressing no β_2 integrin were processed in parallel and used as negative control (all panels).

the transmembrane domain of the heparin-binding epidermal growth factor precursor that serves as DT receptor. The channel forming activity of DT was then substantially decreased when the ectodomain of the DT receptor was attached to the membrane by the GPI anchor (Lanzrein, Sand and Olsnes 1996). In contrast, when the transmembrane and cytosolic domains of an HIV receptor (cluster of differentiation four, CD4) were substituted with the GPI anchor, the mutant CD4 was still able to mediate productive infection by HIV (Diamond *et al.* 1990; Jasin, Page and Littman 1991; Kost *et al.* 1991).

Here we examined the role of the transmembrane segments of the CD11b and CD18 subunits of CR3 in the cell invasive

and pore forming activities of CyaA. Since there is a high degree of homology among the transmembrane segments of the β_2 integrins (Lin *et al.* 2006; Vararattanavech *et al.* 2010), we constructed integrin variants containing artificial transmembrane segments, in order to examine the contribution of the transmembrane segments of CR3 to the cytotoxic activities of CyaA. To ensure the correct anchoring of the integrin variants in the cell membrane and to preserve the dimerization of both integrin subunits, the transmembrane segments of CD11b and CD18 were replaced with transmembrane motifs $L_{23\text{-}7}$ and $V_{6/13E}$, which were previously shown to form dimers in the hydrophobic environment. The motif $L_{23\text{-}7}$, harboring residues L-I-x-x-G-V-x-x-G-V-x-x-T, was previously shown to induce specific dimerization of hydrophobic α-helices of glycophorin A (Lemmon *et al.* 1994). Later, a similar motif, containing residues G-x-x-x-G, was shown to promote dimerization of the integrin α and β subunits (Li *et al.* 2004). The second motif $V_{6/13E}$, consisting of a polyvaline segment and two negatively charged glutamate residues, was previously shown to induce ligand independent dimerization/activation of VEGFR-2 receptor, if the glutamate residues were introduced in an oriented manner (Smith, Smith and Bormann 1996; Bell *et al.* 2000; Dosch and Ballmer-Hofer 2010). The glutamate residues buried in the hydrophobic transmembrane helix in this orientation were also shown to promote ligand independent dimerization of receptor tyrosine kinases (Bell *et al.* 2000), apparently by interchain hydrogen bonding interactions in the hydrophobic lipid bilayer (Gullick *et al.* 1992; Smith, Smith and Bormann 1996; Dosch and Ballmer-Hofer 2010). Using this segment-swapping approach, we demonstrated that the transmembrane motifs $L_{23\text{-}7}$ and $V_{6/13E}$ could also be successfully used for functional heterodimerization of the CD11b and CD18 subunits of the integrin CR3. Using the CD11b-$L_{23\text{-}7}$/CD18-$L_{23\text{-}7}$ and CD11b-$V_{6/13E}$/CD18-$V_{6/13E}$ variants of CR3, we revealed that the amino acid composition of the transmembrane segments of CR3 has no impact on biological activities of CR3-bound CyaA, such as its capacity to translocate the enzymatic AC domain across cellular membrane, or the capacity to form toxin pores and provoke potassium efflux from cells.

To corroborate these observations we next constructed a CR3 variant lacking the transmembrane and cytosolic segments of the CD18 subunit (CD11b/CD18ΔTMC), so that the resulting heterodimer was anchored to the membrane only via the transmembrane α-helix of CD11b. Further, we constructed a CR3 variant with the transmembrane and cytosolic segments of CD11b and CD18 replaced with the GPI anchors (CD11b-GPI/CD18-GPI) that attached the ectodomain of CR3 to the plasma membrane. Both mutant variants were found to be in the extended (high affinity, open) conformation and bound fibrinogen, a natural ligand of CR3. In contrast, the mutant integrins bound CyaA very poorly, compared to native CR3. Since we recently found that CyaA preferentially binds a bent (low affinity, closed) conformation of CR3 (Osicka *et al.* 2015), we hypothesize that the decreased CyaA binding to the mutant integrins was at least in part due to their extended conformation. Moreover, while fibrinogen binds the I-domain of CR3 (Diamond *et al.* 1993), CyaA recognizes the interface between the β-propeller and thigh domain of the integrin (Osicka *et al.* 2015). Thus, an additional explanation of the reduced binding of CyaA to the mutant integrins would be that the deletion of the transmembrane and cytosolic segments of CD18, or the replacement of the transmembrane and cytosolic segments of CD11b and CD18 by the GPI anchor provokes conformational changes in the thigh/β-propeller region and not in the I-domain. Indeed, it was demonstrated that the I-domain of CR3 is correctly folded even when it is expressed as an isolated domain (Michishita, Videm and Arnaout 1993; Lee *et al.* 1995; Huang and Springer 1997). In contrast, folding of the β-propeller/thigh region depends on the integrity of the entire CD11b ectodomain and uses the CD18 subunit as a folding scaffold (Huang and Springer 1997). Thus, the presence and proper orientation of the transmembrane segments of CR3 may be crucial for correct folding of the CyaA-binding site (β-propeller/thigh region), but unimportant for folding of the fibrinogen binding site (I-domain).

Nevertheless, when high concentrations of CyaA were used to compensate for decreased toxin binding efficacy and toxin amounts bound to cells expressing the mutant CR3 variants reached the amounts bound by cells expressing the intact CR3, the cells expressing the mutant integrins were still susceptible to CyaA penetration and pore formation. These activities of CyaA were, however, not restored completely. This indicates that the correct activation state and/or structural integrity of CR3 is also important for a proper positioning of the toxin molecule in respect to the plane of the plasma membrane, so as to enable an efficient toxin penetration into and across the membrane, as required for AC domain delivery and pore formation.

In conclusion, our results demonstrate that the transmembrane α-helices of CR3 do not directly participate in translocation of the AC domain of CyaA across cellular membrane, or in formation of CyaA toxin pores. The results obtained with cells expressing mutant CR3 complexes in which one or both of the transmembrane α-helices have been removed, however, show that a bent conformational state and structural integrity of the β-propeller/thigh region of CR3 is required for toxin binding and subsequent cell-invasive and pore-forming activities of the bound CyaA molecules.

SUPPLEMENTARY DATA

Supplementary data are available at FEMSPD online.

ACKNOWLEDGEMENTS

The authors wish to gratefully acknowledge the excellent technical help of H. Kubinova and S. Charvatova.

FUNDING

This work was supported by the Czech Science Foundation [GAP302/11/0580 to RO], [GAP302/12/0460 to JM] and [GA13-14547S to PS], by the Institute of Microbiology of the CAS, v. v. i. [RVO 61388971], by the Institute of Analytical Chemistry of the CAS, v. v. i. [RVO:68081715] and by the Charles University in Prague [UNCE204025/2012 to AO].

Conflict of interest. None declared.

REFERENCES

Agramonte-Hevia J, Gonzalez-Arenas A, Barrera D *et al.* Gram-negative bacteria and phagocytic cell interaction mediated by complement receptor 3. *FEMS Immunol Med Mic* 2002;**34**:255–66.

Arnaout MA. Structure and function of the leukocyte adhesion molecules CD11/CD18. *Blood* 1990;**75**:1037–50.

Arnaout MA, Gupta SK, Pierce MW *et al.* Amino acid sequence of the alpha subunit of human leukocyte adhesion receptor Mo1 (complement receptor type 3). *J Cell Biol* 1988;**106**:2153–8.

Basler M, Knapp O, Masin J *et al*. Segments crucial for membrane translocation and pore-forming activity of *Bordetella* adenylate cyclase toxin. *J Biol Chem* 2007;**282**:12419–29.

Bell CA, Tynan JA, Hart KC *et al*. Rotational coupling of the transmembrane and kinase domains of the Neu receptor tyrosine kinase. *Mol Biol Cell* 2000;**11**:3589–99.

Benz R, Maier E, Ladant D *et al*. Adenylate cyclase toxin (CyaA) of *Bordetella pertussis*. Evidence for the formation of small ion-permeable channels and comparison with HlyA of *Escherichia coli*. *J Biol Chem* 1994;**269**:27231–9.

Blaustein RO, Koehler TM, Collier RJ *et al*. Anthrax toxin: channel-forming activity of protective antigen in planar phospholipid bilayers. *P Natl Acad Sci USA* 1989;**86**:2209–13.

Bumba L, Masin J, Fiser R *et al*. *Bordetella* adenylate cyclase toxin mobilizes its beta2 integrin receptor into lipid rafts to accomplish translocation across target cell membrane in two steps. *PLoS Pathog* 2010;**6**:e1000901.

Campbell ID, Humphries MJ. Integrin structure, activation and interactions. *Cold Spring Harbor Perspect Biol* 2011;**3**:a004994.

Confer DL, Eaton JW. Phagocyte impotence caused by an invasive bacterial adenylate cyclase. *Science* 1982;**217**:948–50.

Corbi AL, Kishimoto TK, Miller LJ *et al*. The human leukocyte adhesion glycoprotein Mac-1 (complement receptor type 3, CD11b) alpha subunit. Cloning, primary structure and relation to the integrins, von Willebrand factor and factor B. *J Biol Chem* 1988;**263**:12403–11.

Diamond DC, Finberg R, Chaudhuri S *et al*. Human immunodeficiency virus infection is efficiently mediated by a glycolipid-anchored form of CD4. *P Natl Acad Sci USA* 1990;**87**:5001–5.

Diamond MS, Garcia-Aguilar J, Bickford JK *et al*. The I domain is a major recognition site on the leukocyte integrin Mac-1 (CD11b/CD18) for four distinct adhesion ligands. *J Cell Biol* 1993;**120**:1031–43.

Diamond MS, Springer TA. A subpopulation of Mac-1 (CD11b/CD18) molecules mediates neutrophil adhesion to ICAM-1 and fibrinogen. *J Cell Biol* 1993;**120**:545–56.

Donovan JJ, Simon MI, Draper RK *et al*. Diphtheria toxin forms transmembrane channels in planar lipid bilayers. *P Natl Acad Sci USA* 1981;**78**:172–6.

Dosch DD, Ballmer-Hofer K. Transmembrane domain-mediated orientation of receptor monomers in active VEGFR-2 dimers. *FASEB J* 2010;**24**:32–8.

El-Azami-El-Idrissi M, Bauche C, Loucka J *et al*. Interaction of *Bordetella pertussis* adenylate cyclase with CD11b/CD18: Role of toxin acylation and identification of the main integrin interaction domain. *J Biol Chem* 2003;**278**:38514–21.

Glaser P, Sakamoto H, Bellalou J *et al*. Secretion of cyclolysin, the calmodulin-sensitive adenylate cyclase-haemolysin bifunctional protein of *Bordetella pertussis*. *EMBO J* 1988a;**7**:3997–4004.

Glaser P, Ladant D, Sezer O *et al*. The calmodulin-sensitive adenylate cyclase of *Bordetella pertussis*: cloning and expression in *Escherichia coli*. *Mol Microbiol* 1988b;**2**:19–30.

Goodwin MS, Weiss AA. Adenylate cyclase toxin is critical for colonization and pertussis toxin is critical for lethal infection by *Bordetella pertussis* in infant mice. *Infect Immun* 1990;**58**:3445–7.

Gordon VM, Young WW, Jr, Lechler SM *et al*. Adenylate cyclase toxins from *Bacillus anthracis* and *Bordetella pertussis*. Different processes for interaction with and entry into target cells. *J Biol Chem* 1989;**264**:14792–6.

Greenlee DV, Andreasen TJ, Storm DR. Calcium-independent stimulation of *Bordetella pertussis* adenylate cyclase by calmodulin. *Biochemistry* 1982;**21**:2759–64.

Guermonprez P, Khelef N, Blouin E *et al*. The adenylate cyclase toxin of *Bordetella pertussis* binds to target cells via the alpha(M)beta(2) integrin (CD11b/CD18). *J Exp Med* 2001;**193**:1035–44.

Guermonprez P, Ladant D, Karimova G *et al*. Direct delivery of the *Bordetella pertussis* adenylate cyclase toxin to the MHC class I antigen presentation pathway. *J Immunol* 1999;**162**:1910–6.

Gullick WJ, Bottomley AC, Lofts FJ *et al*. Three dimensional structure of the transmembrane region of the proto-oncogenic and oncogenic forms of the neu protein. *EMBO J* 1992;**11**:43–8.

Hackett M, Guo L, Shabanowitz J *et al*. Internal lysine palmitoylation in adenylate cyclase toxin from *Bordetella pertussis*. *Science* 1994;**266**:433–5.

Hasan S, Osickova A, Bumba L *et al*. Interaction of *Bordetella* adenylate cyclase toxin with complement receptor 3 involves multivalent glycan binding. *FEBS Lett* 2015;**589**:374–9.

Hewlett EL, Donato GM, Gray MC. Macrophage cytotoxicity produced by adenylate cyclase toxin from *Bordetella pertussis*: more than just making cyclic AMP! *Mol Microbiol* 2006;**59**:447–59.

Huang C, Springer TA. Folding of the beta-propeller domain of the integrin alphaL subunit is independent of the I domain and dependent on the beta2 subunit. *P Natl Acad Sci USA* 1997;**94**:3162–7.

Hughes PE, Diaz-Gonzalez F, Leong L *et al*. Breaking the integrin hinge. A defined structural constraint regulates integrin signaling. *J Biol Chem* 1996;**271**:6571–4.

Ingalls RR, Arnaout MA, Delude RL *et al*. The CD11/CD18 integrins: characterization of three novel LPS signaling receptors. *Prog Clin Biol Res* 1998;**397**:107–17.

Iwaki M, Ullmann A, Sebo P. Identification by *in vitro* complementation of regions required for cell-invasive activity of *Bordetella pertussis* adenylate cyclase toxin. *Mol Microbiol* 1995;**17**:1015–24.

Jasin M, Page KA, Littman DR. Glycosylphosphatidylinositol-anchored CD4/Thy-1 chimeric molecules serve as human immunodeficiency virus receptors in human, but not mouse, cells and are modulated by gangliosides. *J Virol* 1991;**65**:440–4.

Kagan BL, Finkelstein A, Colombini M. Diphtheria toxin fragment forms large pores in phospholipid bilayer membranes. *P Natl Acad Sci USA* 1981;**78**:4950–4.

Karimova G, Pidoux J, Ullmann A *et al*. A bacterial two-hybrid system based on a reconstituted signal transduction pathway. *P Natl Acad Sci USA* 1998;**95**:5752–6.

Khelef N, Sakamoto H, Guiso N. Both adenylate cyclase and hemolytic activities are required by *Bordetella pertussis* to initiate infection. *Microb Pathogenesis* 1992;**12**:227–35.

Kim M, Carman CV, Springer TA. Bidirectional transmembrane signaling by cytoplasmic domain separation in integrins. *Science* 2003;**301**:1720–5.

Kishimoto TK, O'Connor K, Lee A *et al*. Cloning of the beta subunit of the leukocyte adhesion proteins: homology to an extracellular matrix receptor defines a novel supergene family. *Cell* 1987;**48**:681–90.

Kost TA, Kessler JA, Patel IR *et al*. Human immunodeficiency virus infection and syncytium formation in HeLa cells expressing glycophospholipid-anchored CD4. *J Virol* 1991;**65**:3276–83.

Ladant D. Interaction of *Bordetella pertussis* adenylate cyclase with calmodulin. Identification of two separated calmodulin-binding domains. *J Biol Chem* 1988;**263**:2612–8.

Lanzrein M, Sand O, Olsnes S. GPI-anchored diphtheria toxin receptor allows membrane translocation of the toxin without detectable ion channel activity. *EMBO J* 1996;**15**:725–34.

Lee JO, Rieu P, Arnaout MA *et al*. Crystal structure of the A domain from the alpha subunit of integrin CR3 (CD11b/CD18). *Cell* 1995;**80**:631–8.

Lemmon MA, Treutlein HR, Adams PD *et al*. A dimerization motif for transmembrane alpha-helices. *Nat Struct Biol* 1994;**1**:157–63.

Li R, Gorelik R, Nanda V *et al*. Dimerization of the transmembrane domain of Integrin alphaIIb subunit in cell membranes. *J Biol Chem* 2004;**279**:26666–73.

Lin X, Tan SM, Law SK *et al*. Two types of transmembrane homomeric interactions in the integrin receptor family are evolutionarily conserved. *Proteins* 2006;**63**:16–23.

Lu C, Shimaoka M, Ferzly M *et al*. An isolated, surface-expressed I domain of the integrin alphaLbeta2 is sufficient for strong adhesive function when locked in the open conformation with a disulfide bond. *P Natl Acad Sci USA* 2001;**98**:2387–92.

Luo BH, Carman CV, Takagi J *et al*. Disrupting integrin transmembrane domain heterodimerization increases ligand binding affinity, not valency or clustering. *P Natl Acad Sci USA* 2005;**102**:3679–84.

Michishita M, Videm V, Arnaout MA. A novel divalent cation-binding site in the A domain of the beta 2 integrin CR3 (CD11b/CD18) is essential for ligand binding. *Cell* 1993;**72**:857–67.

Moran P, Raab H, Kohr WJ *et al*. Glycophospholipid membrane anchor attachment. Molecular analysis of the cleavage/attachment site. *J Biol Chem* 1991;**266**:1250–7.

Morova J, Osicka R, Masin J *et al*. RTX cytotoxins recognize beta2 integrin receptors through N-linked oligosaccharides. *P Natl Acad Sci USA* 2008;**105**:5355–60.

Osicka R, Osickova A, Basar T *et al*. Delivery of CD8(+) T-cell epitopes into major histocompatibility complex class I antigen presentation pathway by *Bordetella pertussis* adenylate cyclase: delineation of cell invasive structures and permissive insertion sites. *Infect Immun* 2000;**68**:247–56.

Osicka R, Osickova A, Hasan S *et al*. Bordetella Adenylate cyclase toxin is a unique ligand of the integrin complement receptor 3. *eLife* 2015, DOI: 10.7554/eLife.10766.

Osickova A, Osicka R, Maier E *et al*. An amphipathic alpha-helix including glutamates 509 and 516 is crucial for membrane translocation of adenylate cyclase toxin and modulates formation and cation selectivity of its membrane channels. *J Biol Chem* 1999;**274**:37644–50.

Oxvig C, Lu C, Springer TA. Conformational changes in tertiary structure near the ligand binding site of an integrin I domain. *P Natl Acad Sci USA* 1999;**96**:2215–20.

Pyszniak AM, Carpenito C, Takei F. The role of LFA-1 (CD11a/CD18) cytoplasmic domains in binding to intercellular adhesion molecule-1 (CD54) and in postreceptor cell spreading. *Exp Cell Res* 1997;**233**:78–87.

Sebo P, Fayolle C, d'Andria O *et al*. Cell-invasive activity of epitope-tagged adenylate cyclase of *Bordetella pertussis* allows *in vitro* presentation of a foreign epitope to CD8+ cytotoxic T cells. *Infect Immun* 1995;**63**:3851–7.

Shimaoka M, Lu C, Palframan RT *et al*. Reversibly locking a protein fold in an active conformation with a disulfide bond: integrin alphaL I domains with high affinity and antagonist activity *in vivo*. *P Natl Acad Sci USA* 2001;**98**:6009–14.

Schmid A, Benz R, Just I *et al*. Interaction of *Clostridium botulinum* C2 toxin with lipid bilayer membranes. Formation of cation-selective channels and inhibition of channel function by chloroquine. *J Biol Chem* 1994;**269**:16706–11.

Smith SO, Smith CS, Bormann BJ. Strong hydrogen bonding interactions involving a buried glutamic acid in the transmembrane sequence of the neu/erbB-2 receptor. *Nat Struct Biol* 1996;**3**:252–8.

Takizawa F, Tsuji S, Nagasawa S. Enhancement of macrophage phagocytosis upon iC3b deposition on apoptotic cells. *FEBS Lett* 1996;**397**:269–72.

Tan SM, Hyland RH, Al-Shamkhani A *et al*. Effect of integrin beta 2 subunit truncations on LFA-1 (CD11a/CD18) and Mac-1 (CD11b/CD18) assembly, surface expression and function. *J Immunol* 2000;**165**:2574–81.

Vararattanavech A, Chng CP, Parthasarathy K *et al*. A transmembrane polar interaction is involved in the functional regulation of integrin alpha L beta 2. *J Mol Biol* 2010;**398**:569–83.

Wald T, Petry-Podgorska I, Fiser R *et al*. Quantification of potassium levels in cells treated with *Bordetella* adenylate cyclase toxin. *Anal Biochem* 2014;**450**:57–62.

Weiss AA, Hewlett EL, Myers GA *et al*. Pertussis toxin and extracytoplasmic adenylate cyclase as virulence factors of *Bordetella pertussis*. *J Infect Dis* 1984;**150**:219–22.

Wolff J, Cook GH, Goldhammer AR *et al*. Calmodulin activates prokaryotic adenylate cyclase. *P Natl Acad Sci USA* 1980;**77**:3841–4.

Ye F, Kim C, Ginsberg MH. Molecular mechanism of inside-out integrin regulation. *J Thromb Haemost* 2011;**9(Suppl 1)**:20–5.